High-speed temperature monitoring for steel strips using infrared line-scanners

Rubén Usamentiaga*, Daniel F. Garcia,*, Jesús M. Pérez†

*Department of Computer Science and Engineering, University of Oviedo, Campus de Viesques
33204 Gijón, Asturias, Spain Tel.: +34-985-182626, Fax: +34-985-181986, Email: rusamentiaga@uniovi.es
† ArcelorMittal Global R&D Asturias, 33400 Avilés, Spain, Email: jesus-maria.perez@arcelormittal.com

***Abstract*—Infrared thermography is nowadays used in a wide range of applications. In the steel industry, infrared thermography is mostly used for temperature measurement, which is required for process and quality control. In this work, a high-speed temperature monitoring system for steel strips is proposed. The proposed system is based on infrared line-scanners, which are the most suitable devices for temperature monitoring of moving objects. Accurate temperature measurement is critical for this type of application. Therefore, a rigorous methodology to apply quantitative thermography is presented. In addition, this work proposes accurate temperature and spatial calibrations, including a geometrical model, calibration targets and an optimization procedure. The proposed calibrations open up the possibility of detecting regions of interest in the resulting thermograms, determining the position with accuracy while avoiding distortions. The proposed system is applied to a real industrial application: temperature monitoring in cold rolling. Tests show excellent performance, producing accurate results that provide detailed information about the temperature of very long steel strips.**[1]

***Index Terms*—Temperature measurement, Temperature monitoring, Spatial calibration, Quality control, Infrared line-scanners**

I. Introduction

Infrared thermography (IRT) has become an essential tool in many different fields, including industrial applications [2], physiology [3], inspection of buildings [4] or medical or veterinary applications [5]. In the steel industry, IRT is used to monitor the temperature of machines, facilities and products, which is necessary in order to diagnose and prevent costly failures [6]. In steel production, temperature is one of the most measured variables because achieving the correct temperature is essential in order to obtain the desired metallurgical properties [7].

In steel rolling, temperature monitoring and control is fundamental to produce high-quality products. In this industrial process, metal stock is passed through several pairs of rolls in stands. This procedure has many different objectives, from a reduction of thickness to hardening and improving ductility. When the temperature reached during rolling is above the recrystallization temperature of the metal, the industrial process is referred to as hot rolling, otherwise it is called cold rolling. Many parameters need to be accurately controlled to achieve the desired results of thickness and temperature, such as rolling strength and speed. To this end, complex rolling models have been developed [8], [9]. Temperature is one of the most crucial variables, and it must be measured accurately in order to apply these models. For example, in order to achieve the desired temperature at the exit of the last stand, the global speed of the mill can be changed and cooling sprays can be activated [10]. Therefore, speed and cooling can be used as actuators [11]. Moreover, increasing speed also increases the production rate and the temperature, which can be compensated for with sprays that cool the strip.

The increased demand in steel strips in recent decades, and the constant requirement for high efficiency and availability has significantly increased rolling speeds. Therefore, temperature control during rolling requires improved cooling, but also high-speed temperature monitoring for steel strips. The de facto standard for temperature measurement in rolling mills is the infrared line-scanner (IRLS). These devices are designed for continuous operation in very harsh and dirty industrial environments, where elements such as dust, oil, or water are often present. An IRLS measures the infrared radiation emitted by the steel strips and converts the signal to temperature. The measurement procedure scans the strip while it is moving forward during rolling. Nowadays, an IRLS can produce infrared line-scans consisting of more than 1000 points per scan at 2000 Hz. Thus, IRLS devices are the preferred devices when high-resolution thermograms of moving targets are required. The resulting thermograms, 2D infrared images that contain surface temperature measurements, provide high-resolution information about the temperature of the steel strip after or during rolling. High-resolution in the images provides the opportunity for improved optimization of the industrial thermal processes, detecting small temperature differences across sections of the strips.

In this work, a high-speed temperature monitoring system for steel strips is proposed. The proposed system provides real-time thermogram reconstruction for steel strips during rolling using an IRLS for temperature acquisition. In order to build the thermogram accurately, two different calibrations are considered: temperature calibration and spatial calibration. Temperature calibration is performed using the reference method. Spatial calibration is performed using a geometrical model and an efficient optimization procedure. The proposed procedure requires observation of an especially designed calibration target. Two options are considered and compared: a calibration

[1]This is an extended version of the paper presented at the IEEE IAS Annual Meeting 2019 in Baltimore [1]

target using an electrical heating cable, and a calibration target with emissivity differences. This latter approach is based on a novel design for calibration targets: patterns printed on an aluminum composite. This work compares the performance of the two rules, the complexity required to build them and the obtained accuracy. The spatial calibration of infrared devices is more complex than the calibration with regular cameras because IRLS require distinguishing features in terms of infrared radiation. Moreover, the required temperature of the calibration target is high as, generally, IRLS are only designed for high-temperature measurement. All these challenges are addressed in this work. The proposed procedures are designed to be highly accurate, an indispensable requirement for the steel industry. Moreover, the thermogram reconstruction is designed to be applied under real-time constraints at a high line-scan rate. The proposed system is applied to a real scenario: cold steel rolling in a fast mill. Applications of high-speed temperature measurement are proposed in this environment, including the detection of periodical patterns and frequency analysis.

This paper is organized as follows: Section II presents the correct setup and methodology for temperature measurements and quantitative infrared thermography in industrial environments; Section III presents the proposed approach for thermogram reconstruction of steel strips and calibration using IRLS; Section IV discusses the results obtained, and finally, Section V reports conclusions.

II. Quantitative Infrared Thermography

In order to perform accurate temperature measurements using infrared thermography, a rigorous setup and an understanding of the measurement procedure is required. An IRLS, or any other infrared measuring device, performs a conversion from the measured infrared radiation to temperature. However, the total radiation measured by the IRLS comes from different sources, not only the steel strip. Therefore, recognizing the sources and the influencing factors, such as the physical attributes of the steel strip, is of utmost importance in order to perform accurate temperature measurements that lead to robust decision-making.

Temperature profiles acquired by the IRLS measure the total radiation received by IRLS (W_{tot}) for every single point. This value comes from three different sources: the emission of the target object (E_{obj}), the emission of the surroundings and reflected by the object (E_{refl}), and the emission of the atmosphere (E_{atm}). It can be expressed as (1).

$$W_{tot} = E_{obj} + E_{refl} + E_{atm} \tag{1}$$

The total radiation intensity emitted by an object is described by the Stefan-Boltzmann law (2), and greatly depends on the temperature (T), but also on the emissivity of the object (ε), which is defined as the ratio of the radiant energy emitted by the body to the radiation which would be emitted by a blackbody at the same temperature. The value of σ is constant.

$$W = \varepsilon \cdot \sigma \cdot T^4 \tag{2}$$

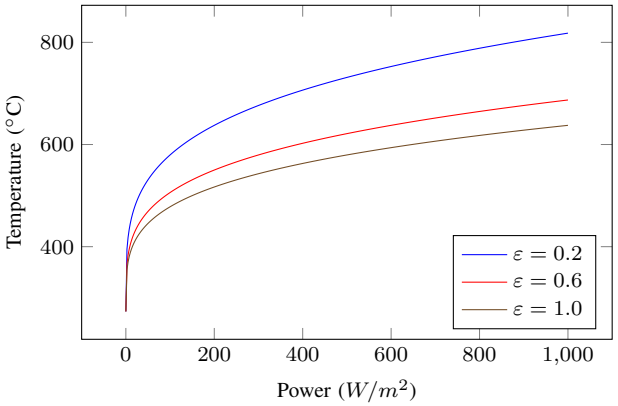

Fig. 1. Conversion from radiation to temperature for different values of emissivity.

Fig. 1 shows the relation between radiation and temperature for different values of emissivity. As can be seen, decreasing the emissivity increases the resulting temperature.

The emission of the target object can be calculated using (2). However, part of the emission is absorbed by the atmosphere, which is described using the transmittance (τ_{atm}). Thus, the emission of the target object can be expressed as (3).

$$E_{obj} = \varepsilon_{obj} \cdot \tau_{atm} \cdot \sigma \cdot (T_{obj})^4 \tag{3}$$

Considering that opaque objects also reflect infrared radiation, the emission of the surroundings and reflected by the object can be expressed as (4), where $1-\varepsilon_{obj}$ is the reflectivity of the object (for opaque objects), and T_{refl} is the reflected temperature.

$$E_{refl} = (1 - \varepsilon_{obj}) \cdot \tau_{atm} \cdot \sigma \cdot (T_{refl})^4 \tag{4}$$

Finally, the emission of the atmosphere is expressed as (5), where $1 - \tau_{atm}$ is the emittance of the atmosphere and T_{atm} is the ambient temperature.

$$E_{atm} = (1 - \tau_{atm}) \cdot \sigma \cdot (T_{atm})^4 \tag{5}$$

In temperature measurements in industrial applications, where the IRLS is very close to the inspected object, the influence of E_{atm} can be considered negligible. Thus, it is normally not considered for the calculations. The influence of E_{refl} depends on the reflectivity of the object of interest, which is high for polished materials and low for oxidized metals. When T_{obj} is much higher than T_{refl}, the influence of E_{refl} in the conversion is also low.

Accurate emissivity measurement is of utmost importance in all scenarios, but especially when measuring temperatures in low-emissivity materials, because the non-linear relation between the temperature and the emitted infrared radiation causes large variations in the resulting temperatures for slight variations in the chosen emissivity [12]. This is the case found in polished steel, which is the most common material in the steel industry.

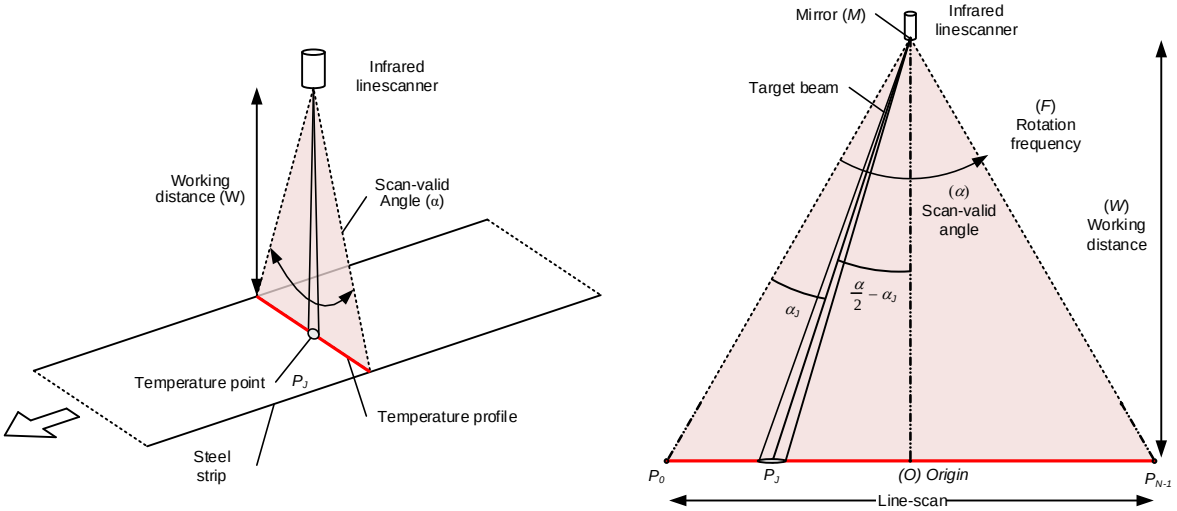

Fig. 2. Geometrical model of the IRLS.

The procedure for the measurement of the emissivity of a material is described in ASTM [13] and ISO [14] standards. The most straightforward approach is the reference emissivity material method. This method requires reference material, that is, pieces of material similar to those where real temperature measurements are performed. These materials are heated with a piece of electrical tape with known emissivity stuck on the surface. The reference temperature on the electrical tape is used to measure the emissivity of the surface of the material by changing the configuration of the emissivity. This procedure must be repeated with as many different materials as required.

The procedure described in the standards for the measurement of the emissivity is only valid for low temperatures. In the case of high temperatures, a different temperature reference is needed. Another option is to obtain the temperature reference from a position where the emissivity is known, such as a hole in the material. When the hole in the material is at least 7 times deeper than the diameter, and the object has a homogeneous temperature all the way through, the radiation exiting from this hole will have an effective emissivity extremely close to 1.0. In this case, the hole can be used as the reference, rather than using electrical tape. Following this approach, it is important to verify that the infrared device can optically resolve the hole for measurement purposes.

The emissivity depends on the angle between the camera and the surface of the object. Therefore, the measurement of emissivity should be performed in similar angle conditions as during real measurements. Variations of less than 30° are negligible, but larger variations cause the emissivity to fall drastically, leading to large variations in the resulting temperature readings.

There are two standard methods to measure the reflected temperature: the reflector method and the direct method [14], [15]. The most common is the reflector method, where a gold metallic coating is placed in the field-of-view of the camera and the temperature is measured assuming an emissivity of 1 and a distance of 0. However, this method requires placing the reflector close to the position of the object of interest. In an industrial application, this is not always possible. Even when this experiment can be performed, the position of the object of interest may be difficult to reach. Thus, the recommended approach in this case is the direct method, where the infrared device is used to measure the temperature of the objects in the scene that are reflected on the object of interest.

III. Proposed Approach for Temperature Monitoring

The proposed system for temperature monitoring uses an IRLS. Before the reconstruction of the thermogram using the acquired line-scans or temperature profiles, radiation measurements must be converted to temperature readings, which requires measurement of emissivity. Moreover, the spatial position of each point in the line-scans must be determined, which requires spatial calibration and definition of the geometric model.

A. Calibration

The conversion from radiation to temperature requires information about the emissivity of the inspected material, in this case, steel. The proposed experiment to determine the emissivity compares the obtained temperature using the IRLS with the temperature provided by a calibrated contact thermometer. The emissivity of the IRLS is modified until both temperature readings are the same. The resulting emissivity is the required configuration parameter in order to perform accurate temperature measurements. This procedure follows the reference method, where the temperature provided by the contact thermometer is used as the considered reference.

Spatial calibration of the IRLS is required to obtain geometric information from the acquired line-scans. The calibration provides a mapping between points in the line-scans and

spatial positions across the inspected steel strip. The proposed calibration is divided into two phases: 1) definition of a theoretical geometrical model for the acquisition of a temperature profile; 2) estimation of the parameters of the proposed model using observations of a calibration target and an optimization procedure.

B. Geometrical model of the IRLS

An IRLS is built using a pyrometer and a motorized mirror. The rotating optics provide a line-scan or temperature profile consisting of multiple measurement points within a scan valid angle. Thus, a sequence of points is measured across a line of the strip. The thermogram is formed as the steel strip moves forward along the roll path. The proposed geometrical model for the IRLS can be seen in Fig. 2.

The geometrical model considers a line-scan consisting of N points, from P_0 to P_{N-1}. The main parameters of the model are: the working distance (W), which is the distance from the IRLS to the inspected object; the rotation frequency of the IRLS (F), which is the same as the line-scan acquisition rate; and the scan valid angle (α), which is the part of the rotation where the temperature measurement is performed. The objective of the spatial calibration is the calculation of the distance from any point in the line-scan to a predetermined origin (O), which can correspond to the center of the line-scan or to a reference point in the rolling mill.

The acquisition period can be calculated from the rotation frequency, F. However, only within the scan valid angle α, is temperature measurement carried out. The period of time, t, can be calculated using (6). The time at which temperature point P_j is acquired, t_j, can be calculated as a fraction of the total acquisition time using (7).

$$t = \frac{\left[\frac{1}{F}\right]}{\frac{2\pi}{\alpha}} = \frac{\alpha}{2\pi F} \tag{6}$$

$$t_j = \frac{j}{N} t \tag{7}$$

The angle at which temperature point P_j is acquired can also be calculated as a fraction of the scan valid angle using (8). This angle can also be determined using (9), where t and F disappear from the model calculations.

$$\alpha_j = \frac{t_j}{t}\alpha \tag{8}$$

$$\alpha_j = \frac{\frac{j}{N}t}{t}\alpha = \frac{j}{N}\alpha \tag{9}$$

Using the angular position of the temperature point j, $\overline{P_jO}$, the distance from the origin, O, to the temperature point, P_j, can be calculated using (10). Substituting the value of α_j in this equation gives (11).

$$\overline{P_jO} = W \tan\left(\frac{\alpha}{2} - \alpha_j\right) \tag{10}$$

$$\overline{P_jO} = W \tan\left(\left[\frac{1}{2} - \frac{j}{N}\right]\alpha\right) \tag{11}$$

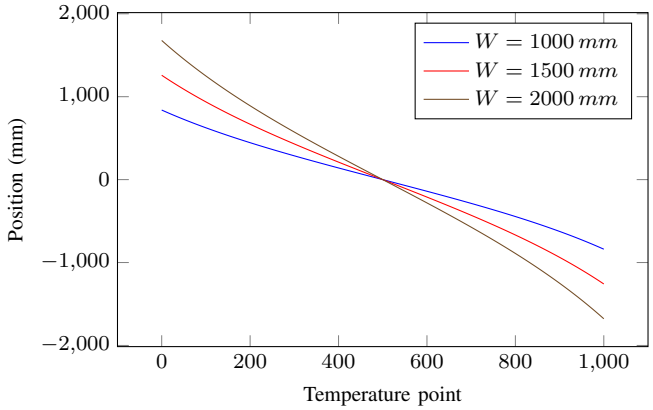

Fig. 3. Spatial position of temperature points in the line scan.

The spatial position, p_j, of any temperature point, j, in the line-scan can be calculated using (12).

$$p_j = \overline{P_jO} \tag{12}$$

Fig. 3 shows the calculated distances using the proposed model for different values of the working distance. As can be seen, increasing this value increases the field of view but also decreases the resolution.

In cases where the center of the line-scan does not match the origin of the reference system, the spatial position of points can be calculated using (13), where C_x represents the distance from the center of the line-scan to the origin.

$$p_j = C_x + W \tan\left(\left[\frac{1}{2} - \frac{j}{N}\right]\alpha\right) \tag{13}$$

C. Estimation of the model parameters

Three parameters are required in the model for the calculation of the spatial position of points:

- Scan angle, α.
- Working distance, W.
- Distance from the center of the line-scan to the origin, C_x.

These three parameters can be roughly estimated. The scan angle is a parameter of the IRLS, and is provided by the manufacturer. The working distance can be measured after the installation of the sensor. The offset of the center of the line-scan to the origin can also be determined from the installation. However, only with an accurate estimation of these parameters can the spatial calibration provide the spatial position of the points with accuracy. The accuracy of this geometric information is crucial for detecting the position and size of hot regions in the steel strips in real working coordinates. This way, rolling control can take the precise correcting measures to address thermal problems.

The proposed procedure for the estimation of the parameters of the model is the observation of known calibration targets. Certain features from the target are then used to estimate the parameters using an iterative optimization procedure. The

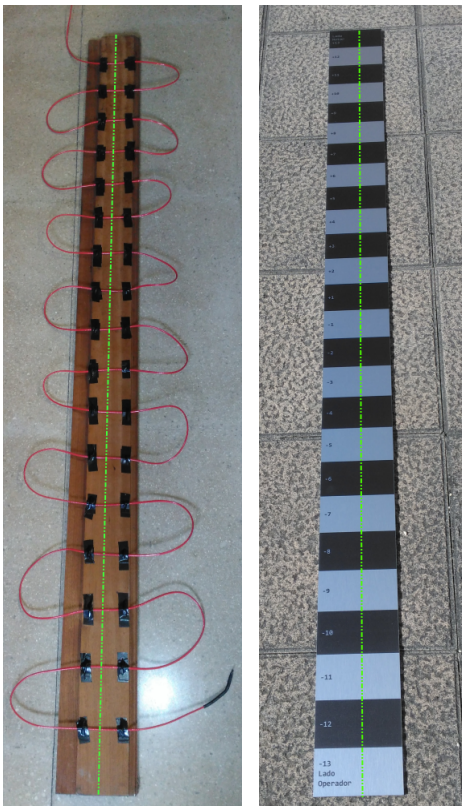

(a) (b)

Fig. 4. Proposed calibration targets. (a) Calibration target based on heating cable. (b) Calibration target based on emissivity differences.

objective of the optimization procedure is to find the vector (α, W, C_x) that minimizes equation (14), where M is the number of observations. This problem, similar to camera calibration, can be solved using nonlinear least-squares methods [16].

$$\min_{\alpha,W,C_x} \left(\sum_{i=1}^{M} \left| p_i - C_x - W \tan\left(\left[\frac{1}{2} - \frac{i}{N} \right] \alpha \right) \right|^2 \right) \quad (14)$$

D. Calibration targets

A calibration target for infrared devices is more difficult to build than a calibration target for a camera, as colors or shades of gray cannot be perceived in the infrared spectrum. Features in the calibration target must be distinguishable by an IRLS that can only perceive temperature difference in a specific range. A naive approach can be carried out using a hot object that is moved in the field of view of the IRLS. However, this approach presents uncertainties in the positioning of the calibration object, which will surely affect the accuracy of the resulting calibration. In this work, two different calibration targets are proposed in order to provide accurate calibrations for an IRLS: a calibration target based on an electric heating cable, and a calibration target based on emissivity differences.

The two proposed calibration targets can be seen in Fig. 4. The first calibration target uses an electric cable that is heated when connected to electricity. This type of cable is very

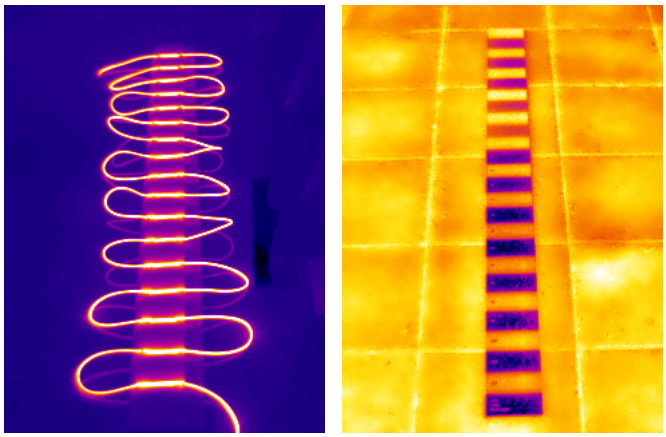

(a) (b)

Fig. 5. Infrared images of the proposed calibration targets. (a) Calibration target based on heating cable. (b) Calibration target based on emissivity differences.

common, as it is installed in electric radiant floor heating systems. The heating cable is only 1/8" thick and very flexible. Thus, it is possible to create different shapes with the cable. In the proposed calibration target, the twisted heating cable is attached to a wooden board using rivets with a particular separation (100 mm), as can be seen in the image. A line-scan acquired parallel to the wooden board, just between the cables, can observe the temperature of the cable at multiple points. The dotted vertical line in Fig. 4a represents the position where the line-scan must be acquired. The position of these points is known, as the cable has been attached with accuracy. Thus, these control points can be used to estimate the coefficients of the mathematical model.

A different approach is proposed for the second calibration target: a calibration target with a combination of materials with different emissivities [17]. The proposed solution is to print the calibration pattern on aluminum composite material. The emissivity of the ink and the emissivity of the aluminum composite material are different (0.83 for the ink and 0.67 for the aluminum panel). Thus, they can be distinguished in the infrared spectrum, even when the two materials are at the same temperature. The material used for the calibration target is Dibond®, a material used for building advertisement boards. Dibond® panels are extremely flat, have very low thermal expansion, and are inexpensive. Printing on this material requires a specific printer. However, this type of printers is widely available nowadays. In this calibration target, a sequence of dark fringes is printed on the calibration board. In areas where the fringe is not present, the surface of the aluminum composite material can be observed. A line-scan acquired parallel to the board will include the information about radiation differences between the printed and non-printed areas. The dotted vertical line in Fig. 4b represents the position where the line-scan must be acquired. The position of these transition points (ink to panel, and panel to ink) can be detected and used for the estimation of model parameters.

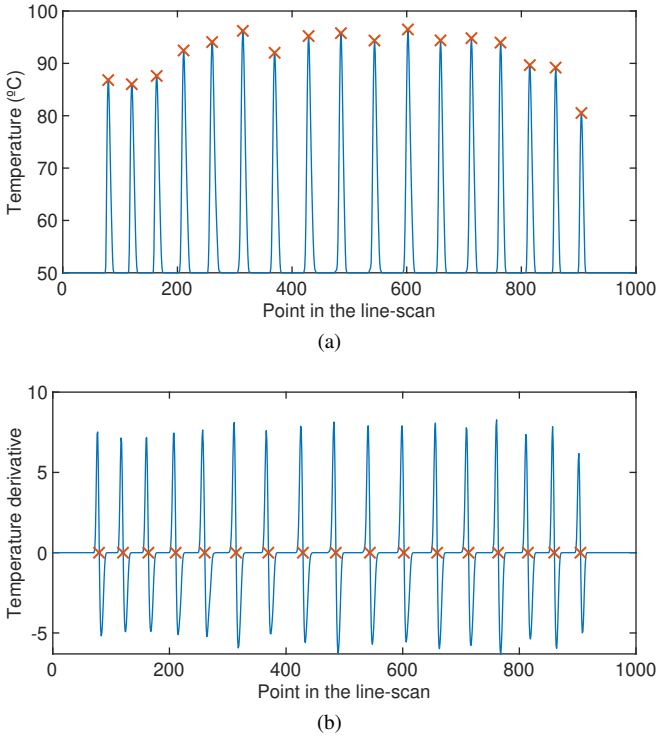

Fig. 6. Extraction of control points in the calibration target based on the heating cable. (a) Line-scan acquired from the calibration target. (b) Derivative of the line-scan.

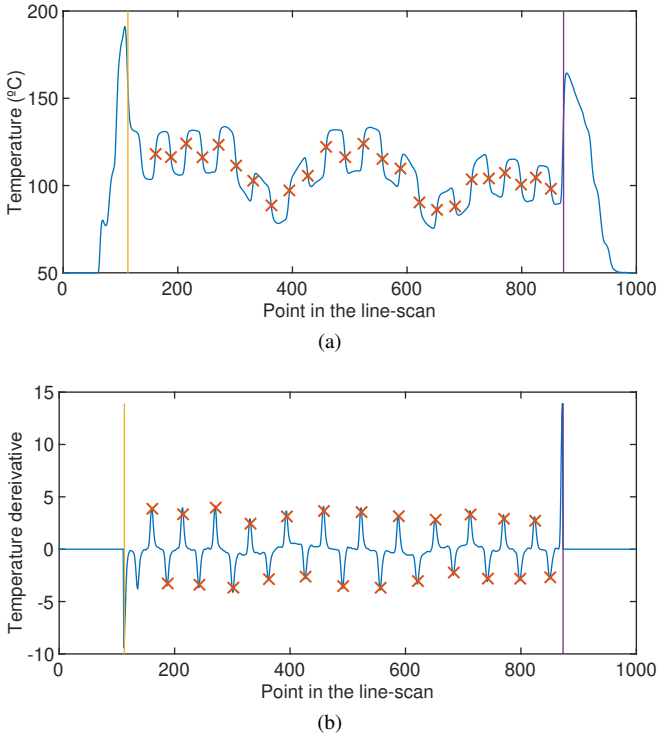

Fig. 7. Extraction of control points in the calibration target based on emissivity differences. (a) Line-scan acquired from the calibration target. (b) Derivative of the line-scan.

Fig. 5 shows infrared images of the two proposed calibration targets. As can be seen, the calibration patterns can be clearly perceived in the infrared spectrum. The first calibration target requires heating. Thus, the heating cable must be connected to electricity in order to be distinguishable using an infrared measuring device. The increased temperature of the heated cable produces a clear contrast with the background. The second calibration target can be observed in the infrared spectrum even without heating. As areas of ink and the aluminum composite material have different emissivity, they also have different reflectivity. Thus, when infrared images of the calibration target are acquired outdoors, the radiation emitted by the sun and the sky produces the thermal contrast in the infrared images due to reflections. When calibration is performed indoors, which is the case in an industrial application, the calibration target must be placed on top of a heater.

E. Extraction of control points

The estimation of the parameters of the geometric model requires the extraction of control points from the observation of the calibration targets. Because the two proposed calibration targets are different, two methods are proposed. In the calibration target based on the heating cable, the objective is to detect the position of the peaks in the line-scan. In the calibration target based on emissivity differences, the objective is to detect the position of the transitions from ink to panel, and from panel to ink.

The proposed procedure for the extraction of the control points in the calibration target based on the heating cable is illustrated in Fig. 6. Fig. 6a show the line-scan acquired when the heating cable is connected to electricity. The objective of the extraction of control points is to calculate the positions marked in the figure, which correspond to the center of the cables. The first step is to calculate the first derivative of the line-scan, as can be seen in Fig. 6b. Possible locations are detected in the derivative signal where it shows a downward zero-crossing, which generally corresponds to the peak maximum. However, noise can cause many zero-crossings. Thus, the derivative is filtered using a Gaussian kernel. Moreover, possible peaks are filtered based on the intensity of the line-scan and the slope. Finally, a neighborhood of points around the resulting peaks is adjusted to a Gaussian profile using curve fitting. The maximum value of these curves corresponds to the positions of the cables in the line-scan.

The procedure to extract the control points in the calibration target based on emissivity differences is slightly different. When this calibration target is used, the position of the control points must be extracted from the transitions between ink and background panel. The procedure is illustrated in Fig. 7. The first step is to determine the boundaries of the calibration target in the line-scan. During calibration, the calibration target must be placed on top of a heater. Thus, the temperature of the heater is higher than the temperature of the rule. The boundaries correspond to the peaks on the left and right of the line-scan. These positions are easily determined, as

they correspond to the maximum and minimum value of the first derivative. The first derivative is also used to detect the transition from ink to panel (high to low), and from panel to ink (low to high). The procedure is the same as that used for the detection of the cables in the other calibration target, but in this case it is used to detect peaks in the derivative, which requires the calculation of a second derivative. Both positive and negative peaks are of interest, as they indicate the positions of the fringe boundaries in the calibration target.

The geometry of the calibration targets is known. Thus, after the extraction of the control points from the calibration targets, a vector of spatial positions and corresponding points in the line-scan is obtained. This map is used to estimate the parameters of the geometric model using the nonlinear optimization procedure. The resulting model can be used to calculate the spatial position of any point in the line-scan.

F. Thermogram reconstruction

An IRLS provides line-scans at a specific acquisition rate. Using the spatial calibration, each point in the line-scan is associated with a position across the width of the roll path where the steel strip is moving. Acquisition of line-scans is repeated while the steel strip moves forward. Thus, each line scan represents a column of the final thermogram, which is associated with a longitudinal position of the strip.

To properly determine the longitudinal position of a line-scan, L_i, the speed, V, of the steel strip is required. Then, the longitudinal position of the line-scan can be calculated using (15), where L_{i-1} is the position of the previous line-scan, and $1/F$ indicates the elapsed time (acquisition period) from the acquisition of the previous line-scan.

$$L_i = L_{i-1} + V\frac{1}{F} \tag{15}$$

Combining the spatial calibration with the longitudinal positioning of the line-scan produces an accurate thermogram reconstruction of the steel strip, where regions of interest such as hot areas are associated with a physical position on the strip. Therefore, the measured information can be used to monitor and control the rolling mill.

IV. Results and Discussion

The proposed temperature monitoring system has been applied to an industrial application: temperature monitoring in a cold rolling mill. Cold rolling produces steel products with increased strength and reduced thickness. During rolling, temperature control is crucial to obtain high-quality flat strips. The temperature monitoring system is installed at the exit of the last stand. Therefore, it provides information about the temperature of the strip after rolling, where obtaining temperature homogeneity is crucial. Temperature is measured using a LandScan IRLS that provides 1000 overlapping measuring points per scan at a frequency of up to 150 Hz in the range 100 to 200°C.

The calibration of the emissivity in the installation is carried out using a temperature reference. A calibrated pyrometer in the installation is used as a temperature reference. Emissivity is varied until both temperature readings match. The final estimated emissivity is 0.37 for the most common steel rolled.

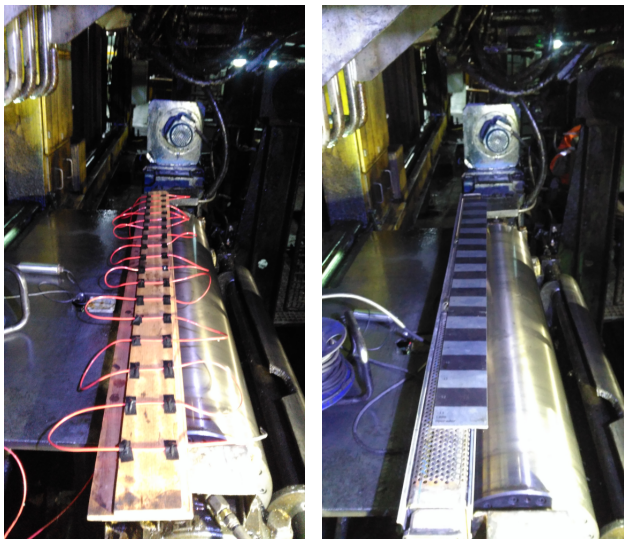

(a) (b)

Fig. 8. Calibration targets during the spatial calibration in the rolling mill. (a) Calibration target based on heating cable. (b) Calibration target based on emissivity differences.

The spatial calibration is performed after the IRLS is installed, as it requires the IRLS to be in its final position. Any displacement of the IRLS from the calibration position would require the calibration to be repeated. Two different spatial calibrations are performed, one using each calibration target. Fig. 8 shows the calibration targets in the rolling mill during the calibration. The IRLS is installed 1 meter above the calibration targets. The center of the calibration target must be positioned at the origin of the rolling mill. This is the reference of the coordinates system across the roll path. This reference is shared with other measuring and control devices in the industrial installation. This position generally corresponds to the center of the rolls.

The first step of the calibration is the acquisition of line-scans. A single line-scan is enough for the proposed procedure. However, a robust average can be calculated when acquiring a sequence of consecutive line-scans from the calibration target. The resulting average-line is then used for the extraction of the control points.

The extraction of control points follows particular procedures depending on the calibration target, as described above. After the extraction, different verifications are performed to detect noise or outlier detections. For example, the number of control points extracted from each target must correspond to the number of control points in that particular target. Moreover, as control points are equally spaced in the calibration target, the positions of the control points in the line-scan must have the same separation.

Control points are used to find the parameters of the geometric model that deliver an optimal value for the objective

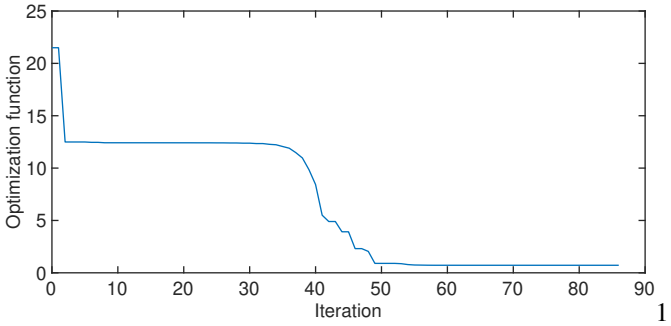

Fig. 9. Optimization function values at each iteration during the estimation of the parameters of the geometrical model.

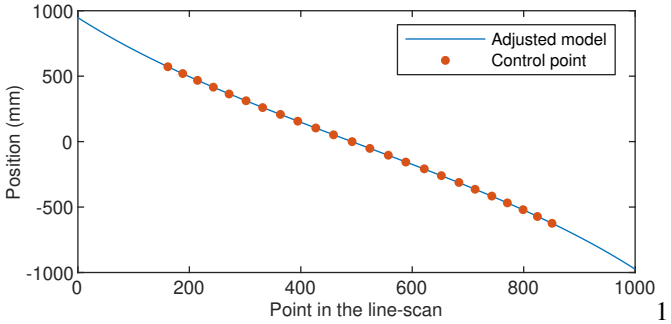

Fig. 10. Adjusted geometrical model after optimization and position of the extracted control points.

function expressed in (14). Two different optimization methods are considered: the Levenberg-Marquardt method [18] based on nonlinear least-squares algorithms, and the simplex search method proposed by Lagarias [19]. The two methods in all the experiments generated the same optimal values. Fig. 9 shows the evolution of the optimization procedure. As can be seen, the optimization procedure finds the parameters of the geometrical model in 50 iterations. The initial values of the parameters are obtained from the IRLS manufacturer (α), and from rough distance approximations obtained in the installation (W, C_x).

Fig. 10 shows the position of control points and the adjusted geometrical model. The calibration procedure accurately determines the optimal values of the geometrical model, which can be used to obtain the spatial position of any point in the line-scan.

The results of the calibration are assessed using two metrics: the root mean square error *RMS*, and the mean absolute error *MAE*. These metrics are defined in (16) and (17), where n is the number of control points, D_i is the measured distance from control point i to the origin, and R_i is the real distance of control point i in the calibration target.

$$RMS = \frac{1}{n}\sum_{i=1}^{n}(D_i - R_i)^2 \tag{16}$$

$$MAE = \frac{1}{n}\sum_{i=1}^{n}|D_i - R_i| \tag{17}$$

TABLE I
ACCURACY RESULTS OF THE SPATIAL CALIBRATION. ALL VALUES ARE GIVEN IN MILLIMETERS

	Calibration target based on	
	Heating cable	Emissivity differences
RMS	2.740	0.719
MAE	1.890	0.617

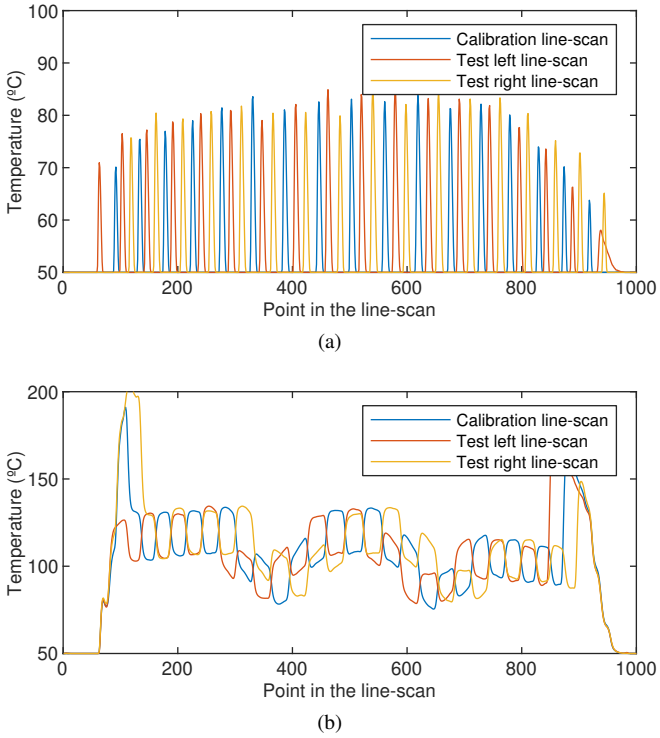

Fig. 11. Line-scans used for testing the spatial calibration. (a) Line-scan acquired from the calibration target based on heating cable. (b) Line-scan acquired from the calibration target based on emissivity differences.

The results of the calibration using the proposed calibration targets can be seen in Table I. As the results in the table indicate, the calibration target based on emissivity differences provides much more accurate results than the calibration target based on heating cable.

Testing the proposed calibration requires the measurement of regions of interest in the field of view of the IRLS. This requires a hot object with known dimensions. The proposed procedure for testing is based on the same calibration target used for calibration, where distances between the extracted control points can be accurately determined. Two new sets of line-scans are acquired by displacing the calibration target to the left and right of the position used for calibration. Fig. 11 shows the line-scans used for testing.

The procedure for the extraction of control points is applied for testing used the acquired line-scans. These coordinates are transformed into physical spatial positions using the adjusted calibration model. The experiment calculates the distance between the control points, which are compared with the real

TABLE II
ACCURACY RESULTS OF THE TESTS. ALL VALUES ARE GIVEN IN MILLIMETERS

	Calibration target based on	
	Heating cable	Emissivity differences
RMS	10.975	1.128
MAE	2.338	0.876
MRE	0.63%	0.40%

distances in the calibration targets. For each control point, the distances to all other controls points are calculated. For example, in the calibration target based on heating cable there are 17 control points. Thus, the number of measured distances in the calibration target is $16 \times 17 = 272$. The experiments for testing the calibration are assessed using the metrics previously used for the calibration (*RMS* and *MAE*). An additional metric, the relative distance error (*MRE*), is proposed to measure the error relative to the measured distance. This metric is defined in (18).

$$MRE = \frac{1}{n}\sum_{i=1}^{n} 100\frac{|D_i - R_i|}{R_i} \tag{18}$$

The results of the testing experiment for the proposed calibration targets is presented in Table II. The results of the calibration target based on emissivity differences is used are much better than the results obtained when using the calibration target based on heating cable. The mean distance error when using the calibration target based on emissivity differences is lower the 1 mm. This calibration result is a great achievement when considering that the spot size of the IRLS is around 10 mm. Using this proposed calibration, the size and position of a possible hot region in the field of view of the IRLS can be determined with an error of only 0.4%, which is more than the required accuracy for the most demanding applications. This also provides a very accurate indication about where rolling control must activate cooling and reduce the temperature of a possible hot region, improving thereby the quality of the resulting steel product.

There is a remarkable difference between the results obtained by the two proposed calibration targets. The reason for this difference in accuracy is related to the construction of the calibration targets. The calibration target based on heating cable is built manually, attaching the cable with rivets to the wooden board. Being a manual procedure, the accuracy when positioning the cables on the board can be greater than 1 mm, which greatly affects the performance of the calibration. Manually made calibration targets severely limit calibration accuracy. Moreover, they are difficult and expensive to build. On the other hand, the calibration target based on emissivity differences is printed on aluminum composite, with no manual intervention. Printing the calibration target not only provides an extremely accurate calibration pattern, it is also inexpensive. Moreover, it can easily be adapted to different requirements such as distances and dimensions.

The calibration pattern based on emissivity differences provides much more accurate results than the calibration target based on heating cable. However, it also has some drawbacks. When the calibration is performed indoors, the calibration targets must be heated in order to distinguish the calibration pattern in the infrared spectrum. Heating the calibration based on heating cable is very easy, as it only requires a standard connection to electricity. On the other hand, heating the calibration pattern based on emissivity differences is much more difficult, as it requires an external heater. Moreover, this external heater must be large enough to cover the whole calibration target (more than 1 m) and provide uniform heating. Such a heater can be difficult to find.

Another disadvantage of the calibration target based on emissivity differences is that it requires more temperature to extract the control points. As can be seen in Fig. 11, the temperature when using this calibration target is much higher. This increased temperature is necessary to distinguish the transition from ink to panel with accuracy. Otherwise, it is not possible to extract the control points required for the estimation of the parameters of the calibration model. Therefore, deciding between the two calibration targets is question of weighing the tradeoff between accuracy and complexity of the calibration procedure.

The calibration is used for the reconstruction of the thermogram. Fig. 12 shows different views of the thermogram of a steel strip after rolling. Fig. 12a shows the complete thermogram, with temperature values in the correct vertical and horizontal position. This thermogram contains 22 410 line-scans each consisting of 1000 temperature points. The thermogram corresponds to a steel strip of 5000 m long and 1 m wide. Fig. 12b shows the enlarged thermogram for a region of 200 m of steel strip where temperature variations can be observed. Fig. 12c shows a virtual pyrometer at the center of the strip. The possibility of creating virtual tools to analyze the temperature of the strip highlights the benefits of having an accurate spatial calibration, as the analysis of the generated information clearly indicates where regions of interest in the strip are located. Fig. 12d shows another of these virtual tools consisting of an average line-scan in the region of strip presented in Fig. 12b.

High-resolution thermograms provide the opportunity for improved analysis and defect detection. Carefully analyzing the thermogram presented in Fig. 12 reveals a periodic thermal pattern. There is a particular temperature variation that repeats over identical space periods. The pattern can be perceived when visualizing an enlarged section of the virtual pyrometer, as can be seen in Fig. 13a. Frequency analysis using the FFT clearly reveals the frequency at which the pattern repeats (Fig. 13b). The pattern repeats every 35 meters. The detection of this pattern demonstrates the advantages of having a high-resolution thermogram.

V. CONCLUSIONS

Temperature monitoring is fundamental in industrial applications. In the steel industry, producing high-quality products

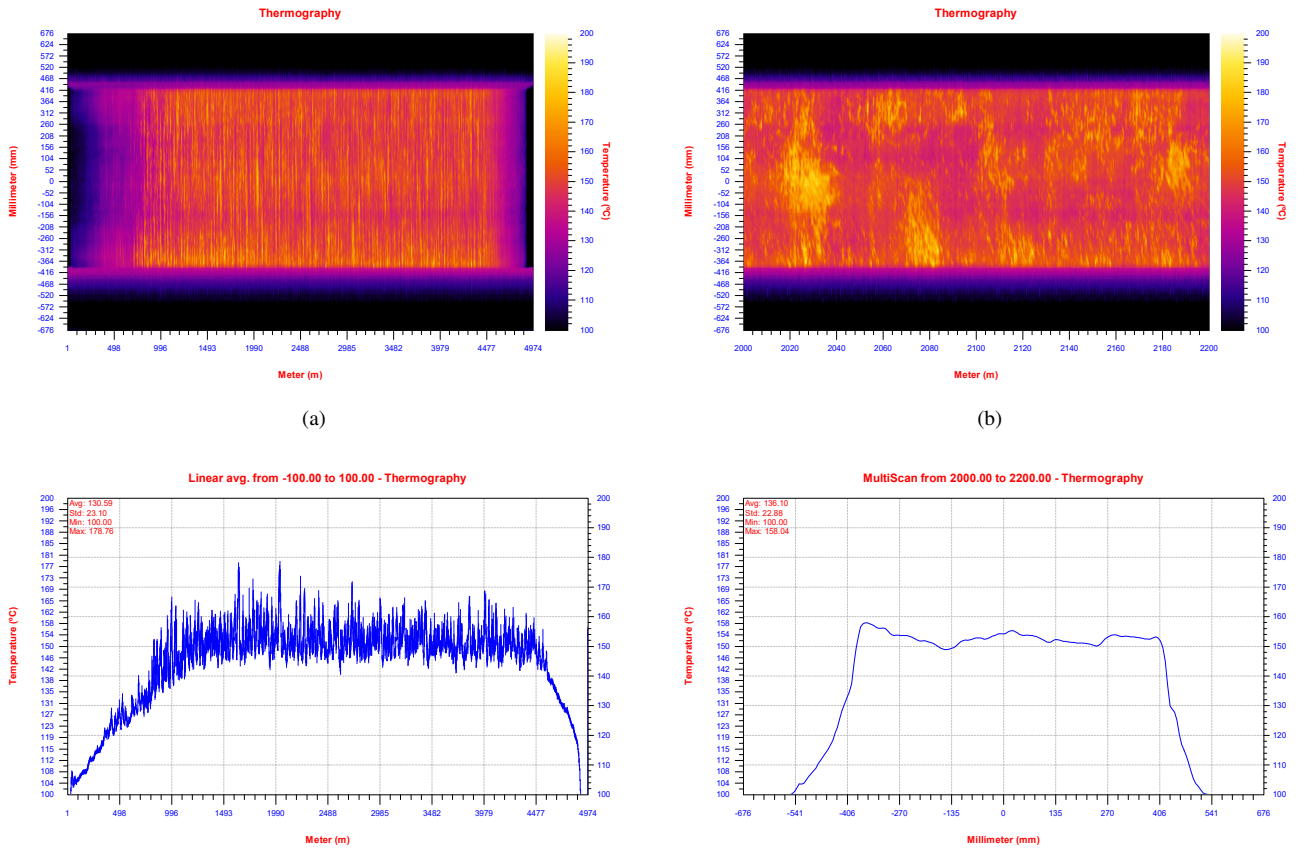

Fig. 12. Reconstruction of the thermogram. (a) Complete thermogram of the steel strip. (b) Enlarged thermogram for a region of 200 m of steel strip. (c) Virtual pyrometer showing the temperature at the center of the strip. (d) Virtual tool showing an average line-scan for a region of 200 m of steel strip.

requires accurate temperature monitoring and control. This work proposes a temperature monitoring system using infrared line-scanners, which are the most common infrared device used for monitoring the temperature of moving objects such as steel strips. In this work, a thorough review of how to apply infrared thermography to temperature measurement in industrial applications is presented. Only by applying a rigorous quantitative approach can infrared thermography provide the required accuracy to control steel manufacturing. This work also describes the most adequate methods to calibrate the temperature compensation procedure. Moreover, a robust and accurate procedure for spatial calibration is proposed. The spatial calibration is required to determine the position of regions of interest in the resulting thermogram, such as hot regions. Two different calibration targets are proposed and compared. A calibration target based on heating cable, which is easy to use in the industrial installation, and a novel design based on emissivity differences, which provides much more accurate results but requires an external heater. This latter calibration target is easy to build, as well as extremely accurate and inexpensive. A thorough search of the relevant literature yielded no previous example of this type of calibration targets for infrared line-scanners, which represents an important contribution to the field.

Tests indicate that the proposed spatial calibration is very accurate when using any of the proposed calibration targets. Measurements provide an average error of less than 1 mm. This is a great achievement considering that the spot size of the infrared line-scanners is around 10 times higher. The obtained accuracy opens up the possibility for the detection of hot regions in the steel strip and the application of very specific cooling to increase product quality. The resulting reconstructed thermogram provides very detailed information that can be used to analyze and detect defects in the manufactured steel strip and periodical thermal patterns. This also underscores the advantages of the proposed system as this information can be used, not only to increase product quality, but also the productivity of the installation.

ACKNOWLEDGEMENTS

This work has been partially funded by the project RTI2018-094849-B-I00 of the Spanish National Plan for Research, Development and Innovation.

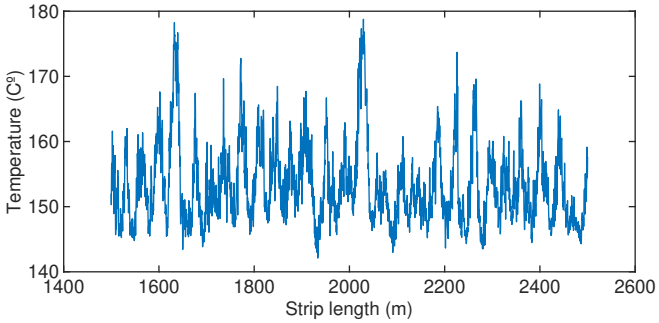

(a)

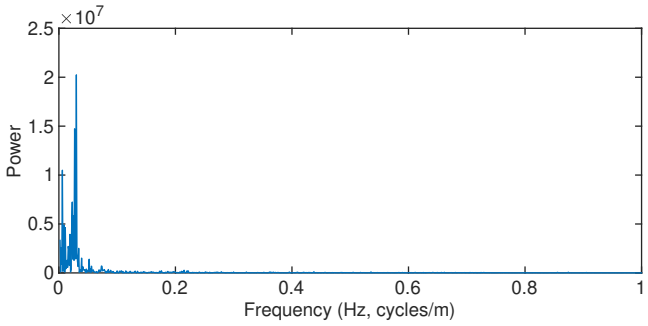

(b)

Fig. 13. Detection of periodic thermal patterns. (a) Enlarged virtual pyrometer showing the temperature at the center of the strip for a region of 1000m of steel strip. (b) FFT of the virtual pyrometer indicating the power for each frequency.

REFERENCES

[1] R. Usamentiaga, D. Garcia, and J. Perez, "High-speed temperature monitoring for steel strips using infrared line-scanners," in *2019 IEEE Industry Applications Society Conference*, vol. 1. IEEE, 2019, pp. 1–8.

[2] R. Usamentiaga, M. Yacine, C. Ibarra-Castanedo, M. Klein, M. Genest, and X. Maldague, "Automated dynamic inspection using active infrared thermography," *IEEE Transactions on Industrial Informatics*, vol. 14, no. 12, pp. 5648–5657, Dec 2018.

[10] G. Hearns, C. Fryer, and P. Reeve, "19 finishing mill predictive temperature control," *Flat-Rolled Steel Processes: Advanced Technologies*, p. 219, 2009.

[3] G. J. Tattersall, "Infrared thermography: a non-invasive window into thermal physiology," *Comparative Biochemistry and Physiology Part A: Molecular & Integrative Physiology*, vol. 202, pp. 78–98, 2016.

[4] T. Hong, C. Koo, J. Kim, M. Lee, and K. Jeong, "A review on sustainable construction management strategies for monitoring, diagnosing, and retrofitting the building's dynamic energy performance: Focused on the operation and maintenance phase," *Applied Energy*, vol. 155, pp. 671–707, 2015.

[5] H. El Hadi, A. Frascati, M. Granzotto, V. Silvestrin, E. Ferlini, R. Vettor, and M. Rossato, "Infrared thermography for indirect assessment of activation of brown adipose tissue in lean and obese male subjects," *Physiological measurement*, vol. 37, no. 12, p. N118, 2016.

[6] R. Usamentiaga, P. Venegas, J. Guerediaga, L. Vega, J. Molleda, and F. Bulnes, "Infrared thermography for temperature measurement and non-destructive testing," *Sensors*, vol. 14, no. 7, pp. 12 305–12 348, 2014.

[7] T. Senuma, "Physical metallurgy of modern high strength steel sheets," *ISIJ international*, vol. 41, no. 6, pp. 520–532, 2001.

[8] M. Grimble and G. Hearns, "Advanced control for hot rolling mills," in *Advances in Control*. Springer, 1999, pp. 135–169.

[9] J. Pittner and M. A. Simaan, "A useful control model for tandem hot metal strip rolling," *IEEE Transactions on Industry Applications*, vol. 46, no. 6, pp. 2251–2258, 2010.

[11] N. S. Samaras and M. A. Simaan, "Optimized trajectory tracking control of multistage dynamic metal-cooling processes," *IEEE Transactions on Industry Applications*, vol. 37, no. 3, pp. 920–927, 2001.

[12] R. Usamentiaga, D. F. Garcia, J. Molleda, F. G. Bulnes, and J. M. Perez, "Temperature measurement using the wedge method: Comparison and application to emissivity estimation and compensation," *IEEE Transactions on Instrumentation and Measurement*, vol. 60, no. 5, pp. 1768–1778, 2011.

[13] ASTM E1933-97, "Standard test methods for measuring and compensating for emissivity using infrared imaging radiometers," 1997.

[14] ISO 18434-1:2008, "Condition monitoring and diagnostics of machines – thermography – part 1: general procedures," 2011.

[15] ASTM E1862, "Measuring and compensating for reflected apparent temperature using infrared imaging radiometers," 1998.

[16] J. Salvi, X. Armangué, and J. Batlle, "A comparative review of camera calibrating methods with accuracy evaluation," *Pattern recognition*, vol. 35, no. 7, pp. 1617–1635, 2002.

[17] R. Usamentiaga, D. Garcia, C. Ibarra-Castanedo, and X. Maldague, "Highly accurate geometric calibration for infrared cameras using inexpensive calibration targets," *Measurement*, vol. 112, pp. 105–116, 2017.

[18] T. F. Coleman and Y. Li, "An interior trust region approach for nonlinear minimization subject to bounds," *SIAM Journal on optimization*, vol. 6, no. 2, pp. 418–445, 1996.

[19] J. C. Lagarias, J. A. Reeds, M. H. Wright, and P. E. Wright, "Convergence properties of the nelder–mead simplex method in low dimensions," *SIAM Journal on optimization*, vol. 9, no. 1, pp. 112–147, 1998.